Received: 9 July 2020 | Revised: 26 October 2020 | Accepted: 28 October 2020

DOI: 10.1111/1556-4029.14634

JOURNAL OF FORENSIC SCIENCES

PAPER

Criminalistics

Convergence-improved congruent matching cells (CMC) method for firing pin impression comparison

Hao Zhang PhD | Jialing Zhu BE | Rongjing Hong PhD | Hua Wang PhD | Fuzhong Sun PhD | Anup Malik

School of Mechanical and Power Engineering, Nanjing Tech University, Nanjing, China

Correspondence
Jialing Zhu, School of Mechanical and Power Engineering, Nanjing Tech University, Nanjing, 211800, China.
Email: jialingzhu@njtech.edu.cn

Funding information
The funding for this research was provided by the National Natural Science Foundation of China (51205211) and the Postgraduate Research & Practice Innovation Program of Jiangsu Province (KYCX20_1002)

Abstract

A firing pin impression is usually concave in shape with a small textured area, which makes it difficult to perform automated algorithm-based comparison. The congruent matching cells (CMC) method was invented for accurate breech face impression comparison, in which a reference impression is divided into correlation cells. Each cell is registered to a cell-sized area of the comparison impression that has maximum similarity in surface topography. Four parameters are used to quantify the congruent matching pattern of the registration position and orientation. This paper aims to further develop the cell-division-matching method based on a convergence feature and to develop practical convergence-improved algorithms for firing pin impression comparison. The convergence feature refers to the tendency of the *x*-*y* registration positions of correlated cell pairs to converge at the correct registration angle when comparing same-source samples at different orientations. The areal Gaussian filter is employed to extract high-frequency micro-features; the least-squares matching method is used to improve each cross-correlation precision and reach convergence in the registration positions of correlated cell pairs; and a density-based clustering algorithm is introduced to collect the registration positions of dense cell pairs relative to a virtual common center and to remove outliers. Improvements are achieved in the reliability and accuracy of the number of congruent matching cell pairs (CMCs) collected, which represents the quantification of the degree of pairwise impression similarity. Experiments in this report used 40 firing pin impression samples on cartridge cases fired from 10 pistols. The results included no false identifications or false exclusions.

KEYWORDS
automated ballistic identification, congruent matching cells, density-based clustering, firing pin impression, least-square matching

1 | INTRODUCTION

During firing, parts of the firearm make strong contact with the bullets and cartridge cases, and characteristic markings of the firearm are transferred onto the surface of the ammunition contributing to permanent changes in its topography. These form a kind of toolmark called "ballistic signatures" [1]. In ballistic examinations, these signatures are compared in detail to assess whether the bullets or casings were fired from a particular firearm [2].

Ballistic examination traditionally relies mainly on highly skilled practitioners and meticulous side-by-side comparisons of toolmarks under a comparison microscope [3,4]. Since the early 1990 s,

[Correction added on January 24, 2021, after first online publication: New funding information details has been added in the article.]

commercial automated ballistic identification systems such as Drugfire [5] and the Integrated Ballistic Identification System (IBIS) [6] have been developed, producing a revolution in the speed at which ballistic toolmark analysis can proceed. With the rapid development of computational technology, automated ballistic identification techniques are becoming a promising means to improve the efficiency and accuracy of ballistic examinations [7–9]. In particular, the latest image processing technology used in pattern recognition or data mining can be systematically applied to the extraction and analysis of feature information of ballistic signatures in order to achieve convincing and accurate qualitative discrimination and even the quantitative comparison of toolmarks. However, the numbers of bullets and cartridge cases found at crime scenes are usually limited, and thus, few impressions may be available for examination as evidence. Comparisons between finite samples are generally classified for object verification rather than latent identification [10,11]. The purpose of this automated procedure is to examine the links between impressions from a crime scene and a suspect's firearm, and to determine whether or not they match, rather than just searching a claimed database for the most similar impression to a latent identity.

An innovative method named congruent matching cells (CMC) has been proposed at the National Institute of Standards and Technology (NIST) to assist examiners in toolmark comparison [12]. The CMC method is based on the principle of discretization. A reference image is divided into correlation cells. Each cell is registered to a cell-sized area of a comparison image that has maximum similarity in surface topography. For each resulting cell pair, one parameter is used to quantify the similarity in cell surface topography and three parameters to quantify the pattern congruency of the registration position and orientation. Cell correlation can effectively improve the accuracy of correlation by eliminating less pertinent regions which contain limited individual characteristics [13].

In ballistic examinations, breech face impressions and firing pin impressions are the most reliable toolmarks found on cartridge cases and are relatively easy to image. The CMC method has been validated using both three-dimensional (3D) topography images and two-dimensional (2D) intensity images of breech face impressions [9,14]. However, due to the small area and paraboloid form of firing pin impressions, challenges arise when the CMC algorithm is applied directly to the analysis of these indentations which include random variations in curvature and depth and relatively content-poor texture. A congruent matching cross-section (CMX) method similar to CMC has been proposed to overcome these challenges [15]. In the CMX algorithm, each firing pin impression is sliced into layers, and the resulting circular cross-sections are transformed into 2D linear profiles using a polar coordinate transformation. Similar to the core idea of the CMC method, cross-correlation is used to quantify the similarity of pairwise profiles which represent the two correlated firing pin impressions. Then three identification parameters with corresponding thresholds are designed to determine the congruency of the pairwise profile pattern. However, the CMX algorithm also has drawbacks. The main problem is that the texture at the bottom cannot be utilized as effectively as other parts of the firing pin impression, although the bottom area may contain information that is more critical.

Highlights

- A convergence-improved congruent matching cells method is proposed for firing pin toolmark analysis.
- The areal Gaussian regression filter is employed to extract the critical micro-topography.
- Least-squares matching method corrects cell correlation against geometric and rotation distortions.
- Density-based clustering achieves congruence enhancement of cell pair registration.
- The improved method successfully separates known-matching and known non-matching samples.

This paper aims to justify the CMC method as an effective practical application in the comparison of firing pin impressions, focusing on several enhancement algorithms to optimize the convergence of the cell-division-matching method. The following sections introduce the basic concept of the convergence-improved CMC method, explain the detailed procedure of the improved algorithm, and present validation experiments and results.

2 | THE CONVERGENCE-IMPROVED CMC METHOD

2.1 | The original CMC method

There are both “valid” and “invalid” regions on the toolmarks of bullets and cartridge cases due to different contact conditions during firing [5]. The valid region refers to a surface portion containing the individual characteristics produced by complete contact between cartridge case and the firearm parts. Conversely, an invalid region refers to poor contact which represents the incomplete transfer of the individual characteristics of the firearm parts. If included in a quantitative correlation between entire areas of pairwise marks, invalid regions may reduce accuracy. To overcome this problem, a discretization-based method named congruent matching cells (CMC) was proposed at NIST [9,12]. In the CMC method, the entire image is divided into small correlation cells so that valid regions can be identified and invalid regions eliminated. During a step-by-step rotated correlation, each cell of the reference marks is registered to a cell-sized area of the comparison image which has maximum similarity in surface topography [14]. For two topographies A and B originating from the same firearm, the cell pairs located in the common valid correlation region can be characterized by:

1. High topography similarity, quantified by, e.g., the normalized maximum areal cross-correlation function $ACCF_{max}$,

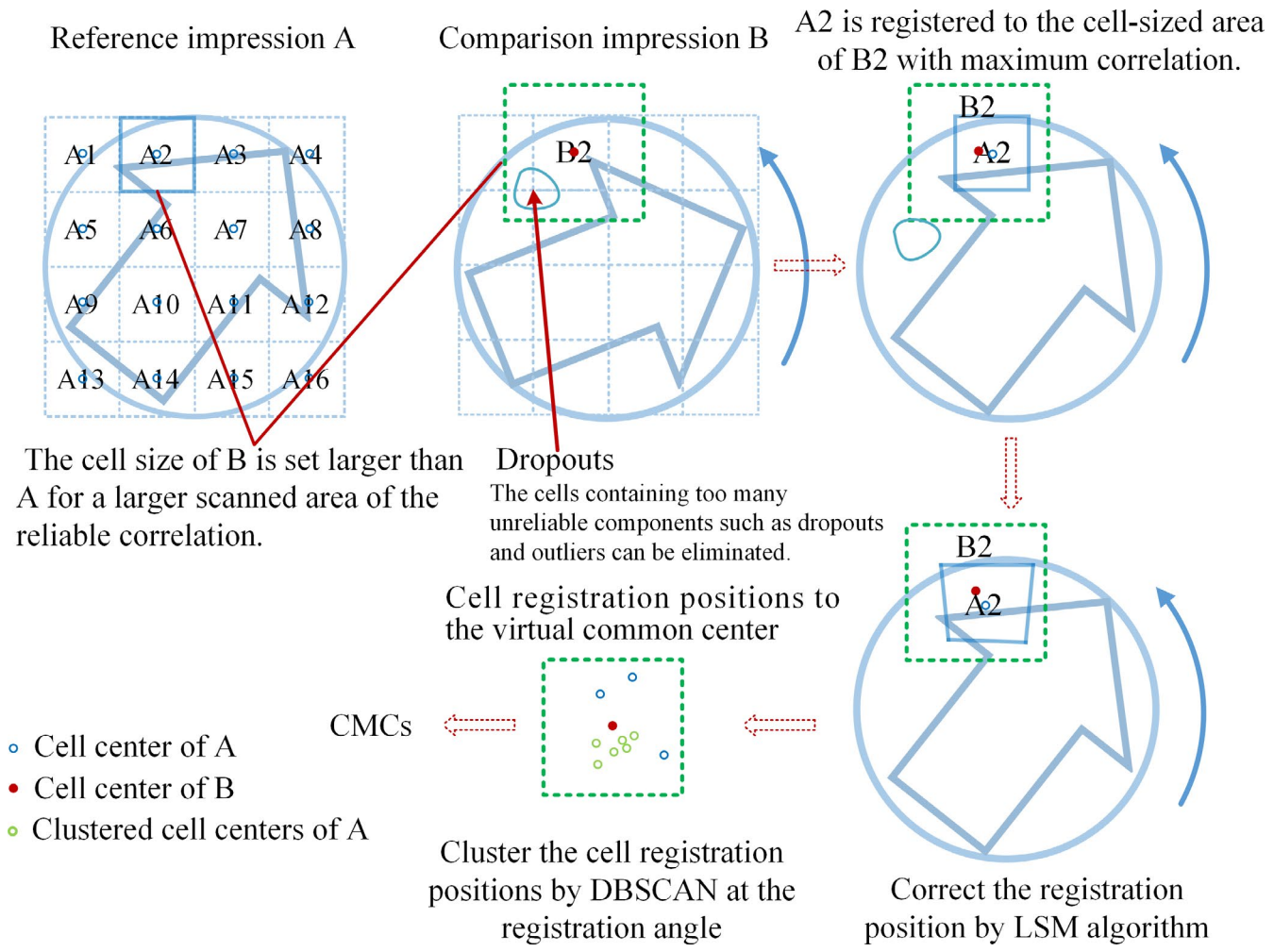

FIGURE 1 Comparison scheme of the convergence-improved CMC method. A2 represents the reference cell and B2 (the green dotted window) represents the comparison cell which is actually set larger than A2. During the correlation process, cell A2 scans B2 in each rotated position of the correlated image B [Color figure can be viewed at wileyonlinelibrary.com]

2. Similar registration angles θ for the cells registered in the comparison image, and
3. Similar *x*-*y* spatial distribution patterns for the cell arrays in both images.

Four identification parameters, $ACCF_{max}$, θ, *x* and *y* with the corresponding thresholds T_{ACCF}, T_{θ}, T_x and T_y, are used to determine the number of congruent matching cell pairs (CMCs) in a pair of images.

2.2 | The convergence-improved CMC method

A convergence feature of the registration positions of CMCs in the CMC algorithm has been discussed by Chen [13]. The convergence feature refers to the tendency of the CMCs' *x*-*y* registration positions to converge to the compared cell center at the correct registration angle. The strength of convergence was proposed as an additional criterion to aid the CMC algorithm in determining CMCs.

Inspired by this feature, a further convergence-improved CMC method is proposed for the comparison of firing pin impressions. When the original CMC method is applied directly to the comparison of indentations in practical applications, it is difficult to obtain clearly distinguishable CMCs to separate matching samples from non-matching samples, which could be due to many factors such as random variations in curvature or depth, relatively content-poor textures, and topography distortions caused by rotation and geometric deformation.

The purpose of the present research is to explore in depth the convergence feature of CMCs, and to develop practical algorithms such as LSM and a clustering algorithm to increase the number of CMCs and remove unreliable registered cells. The convergence-improved CMC algorithm is composed of a series of practical data processing sub-algorithms. The areal Gaussian filter [16] is employed to extract the roughness component from the hemispherically shaped surface so as to highlight the individual characteristics. In order to meet the actual requirements of automated analysis, cell pair correlation in all orientations is used, rather than the nearby orientations of possible correct registration angle estimated by empirical observation. The correlation distortions caused by rotation and geometric deformations are corrected using the LSM method

to guarantee a more reliable registration position of the correlated cell pairs. The density-based clustering algorithm is used to cluster the dense cell pair registration positions relative to a virtual common center, with the aim of collecting more credible CMCs and excluding untrustworthy pairs. In practice, the exclusion of the latter is particularly effective in eliminating false identifications of KNM impression pairs. A comparison scheme of the convergence-improved CMC method is shown in Figure 1.

3 | METHODS

3.1 | Impression measurement and data processing

The convergence-improved method is applied to the impression samples acquired using a Nanofocus µSurf disk-scanning confocal microscope, which allows for the non-destructive acquisition of 3D surface topography [15]. Figure 2A shows a typical 3D topography surface of a firing pin impression. A single field of view of 20× objective is square, with approximate dimensions of 0.8 × 0.8 mm. The raw topography images have 1.56 µm X/Y resolution and consist of 512 × 512 pixels. The z-slice interval is 0.2–0.3 µm and about 400 image slices are measured for a total vertical range of 120 µm.

Limited by the measurement principle of the machine, the raw topography data certainly contains unreliable components such as noise, dropouts, and outliers, which are unfavorable conditions for comparison. By extension, the cell-division-matching algorithm of the CMC method is considered to be more suitable for planar objects than irregular surfaces. Hence, for the practical application of the CMC algorithm to the concave surface of firing pin impressions, three-dimensional filtering is a necessary initial procedure to eliminate unreliable data points and to attenuate shape and waviness. Referring to the CMX method [15], we implemented the same four steps of signal processing, especially the low-pass areal spline filter with a short cutoff wavelength (5 pixels, about 7.81 µm) and the areal Gaussian regression filter with a long cutoff wavelength (60 pixels, about 93.75 µm) to establish a robust mean surface (Figure 2B) for the hemispherically shaped impressions. Then, roughness surface (Figure 3) can be extracted via point-by-point subtraction between the measured topography and mean surface. The purpose here is to extract the critical micro-geometries representing the individual characteristics from the macro-geometries (size, shape, and waviness) representing the class characteristics of certain brands of firearms for better automated analysis [2].

3.2 | Rotation increment analysis and the full range of rotation detection

In the CMC validation experiments [4,9,17,18], since the true matching angle was unknown, the possible registration angle was always estimated in advance based on empirical observations of surface characteristics, and the rotation angle was set within a limited range

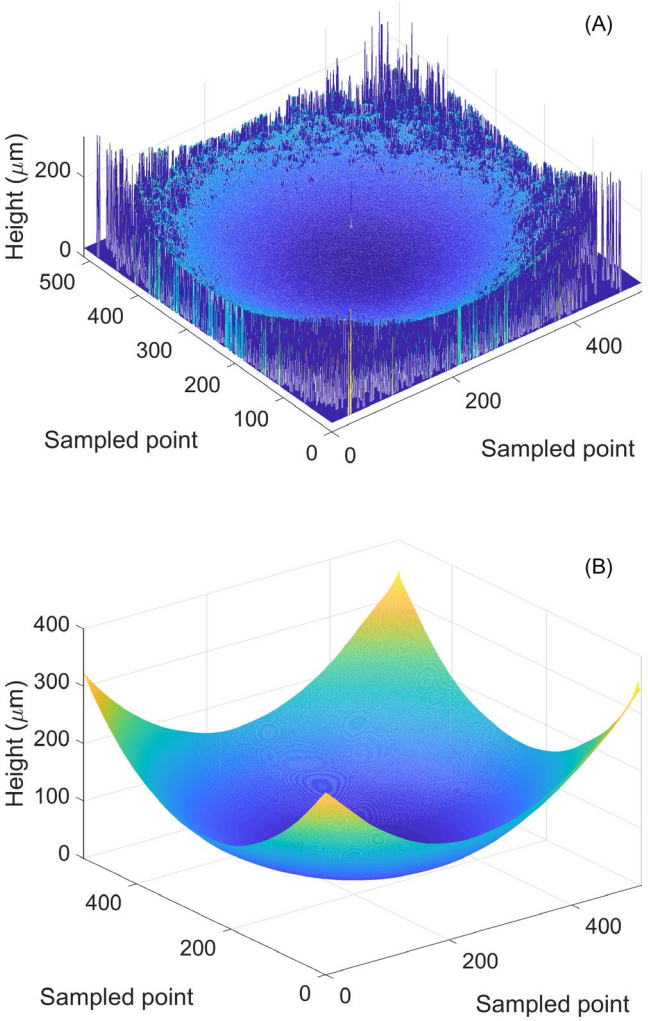

FIGURE 2 Mean surface of a firing pin impression achieved by the Gaussian regression filter: (A) raw data of a typical firing pin impression; (B) mean surface obtained by the areal filter [Color figure can be viewed at wileyonlinelibrary.com]

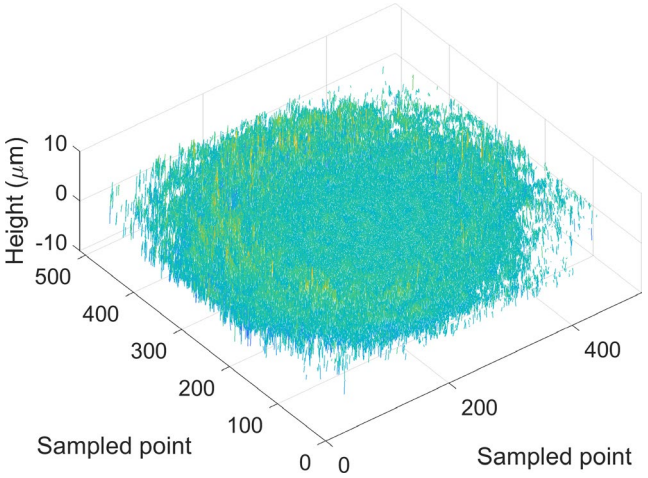

FIGURE 3 Roughness surface obtained by subtraction applied between the measured topography and mean surface [Color figure can be viewed at wileyonlinelibrary.com]

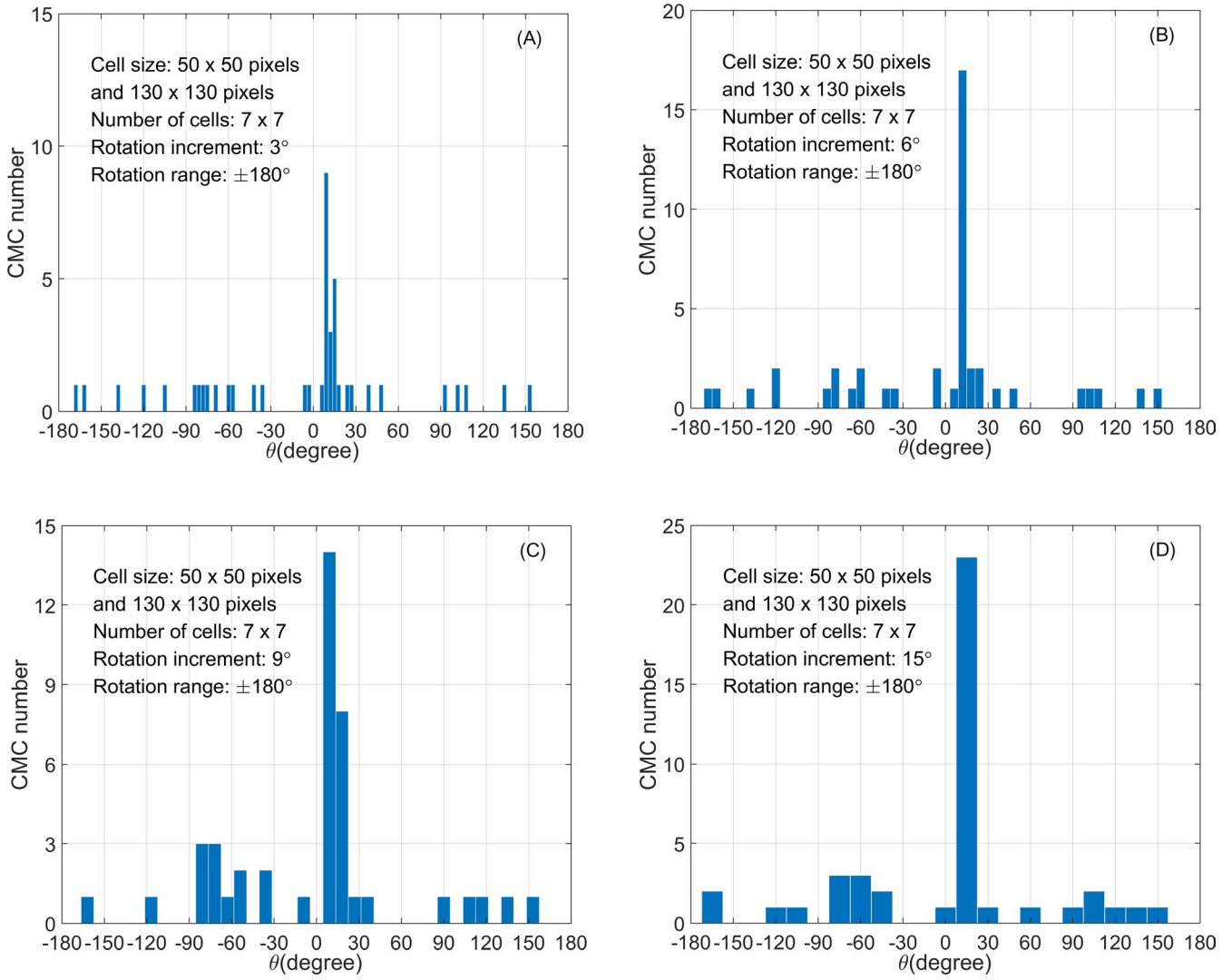

FIGURE 4 CMCs for a KM comparison with different rotation increments of: (A) 3°; (B) 6°; (C) 9°; (D) 15° [Color figure can be viewed at wileyonlinelibrary.com]

such as 30° [9] with respect to the pre-estimated angle, in order to reduce the otherwise large numbers of cross-correlation calculations required. In this paper, however, the rotation correlation should be extended to the full 360° range so as to achieve complete automated ballistic comparison.

Figure 4A–D show the results of the full orientation CMC algorithm with the thresholds set as T_{ACCF} =40% on an example of pairwise KM firing pin impressions with the rotations in 3°, 6°, 9°, and 15° increments. The peak of the CMC number close to the correct registration angle in the CMC-θ distribution pattern is the key parameter used to define the CMCs score and to quantify the similarity of pairwise impressions. The figures show that, under different rotation conditions, the CMC-θ distribution exhibits a certain degree of randomness but the peak appears quite accurately at the discretized registration angle close to the true matching angle. Hence, we can select a relatively large increment to help perform the full-range rotation correlation, with the goal of determining the registration angle. Certainly, if necessary, the search can be further refined in smaller increments to determine a more precise registration angle near the previous registration angle. In this study, the rotation condition is set to the full range of 360° in increments of 15°.

3.3 | Least-squares matching

Theoretically, if two firing pin impressions from the same firearm are registered at the correct matching angle, the cell pairs should satisfy all four parameters threshold settings owing to their strong topography similarity. In practice, some KM impression pairs may be falsely excluded because of two main distortions in firing pin impressions. Firstly, a firing pin impression usually forms a concave plastic deformation when the firing pin strikes. Owing to unpredictable impact conditions such as strike angle, magnitude of striking force, and the strength and microstructure of material, even impressions from the same tool will inevitably undergo geometric deformation (structural change) and depth variations. Secondly, the rotation interval in the implementation of the algorithm will cause an angular offset in most of the pairwise

comparisons, as well as a rotation distortion in the cell pair correlation. The offset and its distortion will worsen as the increment of rotation increases. This also means that the actual registration angle is usually close to, but not exactly equal to, the true matching angle. Hence, the correlation between corresponding cells must take into account such adverse effects as geometric deformation, depth variation, and angular offset.

In order to solve the above-mentioned distortions that affect the reliability of the CMC algorithm, the LSM method is introduced as a preferred approach for amending the cross-correlated results between pairs of cells. LSM is a highly accurate patch matching method which is widely used to correct distortions in perspective as well as geometric deformations and angular deviations. This straightforward solution minimizes the squared sum of residual differences and thus represents the optimum transformation giving the optimal window matching [19,20].

3.3.1 | Least-squares matching model

Assume a pair of correlated cells are $g_1(x_1, y_1)$ and $g_2(x_2, y_2)$ with the same size in two impressions. The affine transformation model can be used to describe the geometric deviation, and the linear model describes the depth variation, as shown in Equation 1,

$$g_1(x_1, y_1) + n_1(x_1, y_1) = h_0 + h_1 g_2(x_2, y_2) + n_2(x_2, y_2) \quad (1)$$

where:

$$\begin{cases} x_2 = a_0 + a_1 x + a_2 y \\ y_2 = b_0 + b_1 x + b_2 y \end{cases} \quad (2)$$

and a_i, b_i are the unknown parameters in the affine transformation model, h_0, h_1 are the unknown parameters in the linear model, and n_1, n_2 represent random instrument noise.

The residual difference is expressed by Equation 3. Based on the theory of the LSM algorithm, the unknown parameters can be obtained by minimizing this equation. To acquire the solution, Equation 3 can be expanded to a linear function with the help of the Taylor expansion.

$$v = g_1(x_1, y_1) - h_0 - h_1 g_2(x_2, y_2) + n_1(x_1, y_1) - n_2(x_2, y_2) \quad (3)$$

$$v = c_1 dh_0 + c_2 dh_1 + c_3 da_0 + c_4 da_1 + c_5 da_2 + c_6 db_0 + c_7 db_1 + c_8 db_2 - \Delta g \quad (4)$$

where $c_1 = 1$, $c_2 = g_2$, $c_3 = \frac{\partial g_2}{\partial x_2}$, $c_4 = x_1 \frac{\partial g_2}{\partial x_2}$, $c_5 = y_1 \frac{\partial g_2}{\partial x_2}$, $c_6 = \frac{\partial g_2}{\partial y_2}$, $c_7 = x_1 \frac{\partial g_2}{\partial y_2}$, $c_8 = y_1 \frac{\partial g_2}{\partial y_2}$, and $\Delta g = n_2(x_2, y_2) - n_1(x_1, y_1)$.

For each pixel element, Equation 4 represents a linearized equation which relates differences in depth to the unknown increments of the eight transformed parameters (dh_0, dh_1, da_0, da_1, da_2, db_0, db_1, db_2). Equation 5 can be rewritten in matrix notation, as:

$$V = CX - L \quad (5)$$

where $X = [dh_0, dh_1, da_0, da_1, da_2, db_0, db_1, db_2]^T$ is the vector of the unknown parameters, and C is the coefficient matrix.

Generally, the matrix function is highly redundant, in which the number of pixels exceeds the number of undetermined parameters, and thus Equation 5 is always solved using the least-squares approach where the squared sum of the depth differences between the correlated cells is minimized. Through an iterative solving process, LSM can achieve an accurate match between two patches against geometric deformation, rotation distortion, and depth variation.

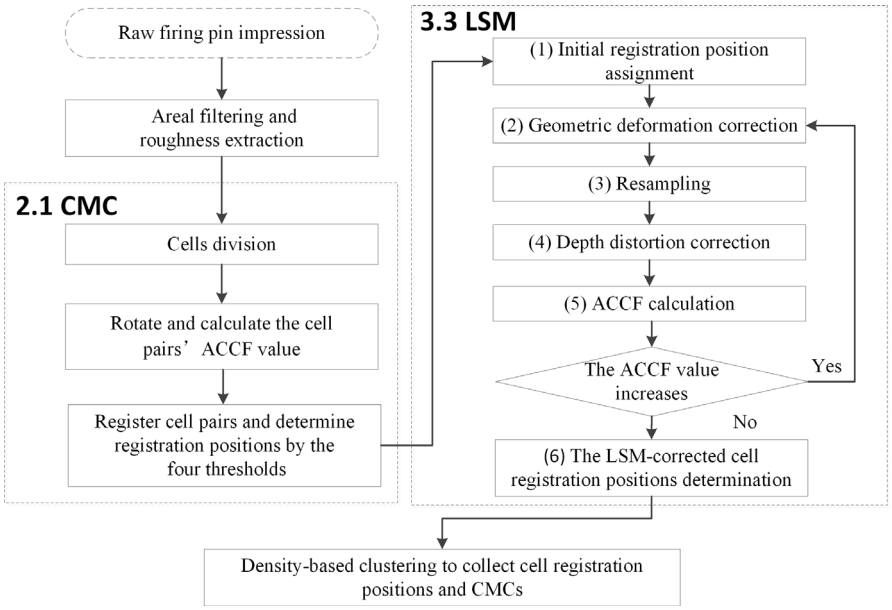

FIGURE 5 Block diagram of the integrated CMC and LSM algorithm

3.3.2 | Improvement of cross-correlation calculation

As mentioned above, the LSM algorithm is proposed to improve cell pair cross-correlation. It serves as a refined matching operation in the CMC algorithm acting against various types of distortion. Figure 5 describes the complete implementation of the integrated CMC and LSM algorithm, with the specific procedures then given below:

1. Initial registration position. Run CMC algorithm, and determine possible registration angle by counting the CMC number. Assign initial registration positions to the registered cell pairs as tentative key points for the optimization solution.
2. Geometric deformation correction. The registered cells of the reference impression are calibrated and transformed into an array of corresponding cells in the comparison impression according to the geometric deformation correction parameters $a_0, a_1, a_2, b_0, b_1, b_2$, and Equation 2.
3. Resampling. Since the transformed coordinates x_2 and y_2 cannot always be integers in the array of compared cells, resampling by bilinear interpolation is a reasonable method to reacquire depth data at integer coordinates.
4. Depth distortion correction. Correct the depth difference of the cells depending on the depth correction parameters h_0 and h_1 obtained by LSM and $h_0 + h_1 g_2(x_2, y_2)$.
5. ACCF calculation. Conduct ACCF again between the corrected cells and the comparison cells after distortion correction. If the correlation value is greater than that of the previous iteration, repeat steps 2, 3, and 4 above; otherwise stop the iteration.
6. Determine the final registration position with the maximum cross-correlation value.

Figure 6 shows the cell registration positions of an example of KM impression pair at the registration angle. The red point represents the virtual common center for all divided cells of the comparison impression. The blue points represent the *x*-*y* registration positions of the registered cells of the reference impression at the registration angle obtained using the original CMC method, while the green points represent the better registration positions in the comparison cells corrected using the LSM algorithm. Due to correction with the LSM method, all of the initial registration positions show noticeable displacements, some of which are relatively large. Through manual comparison and analysis, it is found that the large displacements are always associated with cell pairs which are seriously affected by various types of distortion. The above results indicate that the LSM algorithm can effectively overcome the problems caused by geometric deformation, angular deviation, and depth variation, and improve the cross-correlation scores of cell pairs as well as their congruent pattern.

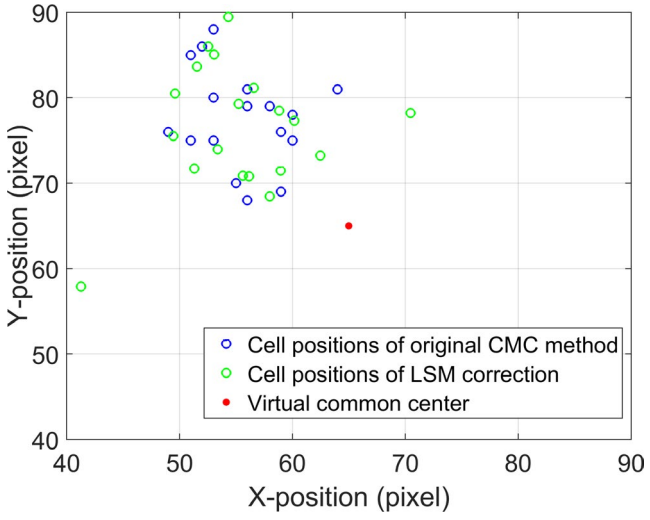

FIGURE 6 Cell registration positions acquired at correct registration angle by the original CMC algorithm and corrected by LSM method [Color figure can be viewed at wileyonlinelibrary.com]

3.4 | Density-based clustering algorithm

According to the cell-division-matching principle, at the correct registration angle of pairwise KM impressions, the *x*-*y* registration positions of most cells should converge in a similar pattern of spatial distribution. Conversely, the *x*-*y* registration positions of the registered cell pairs of KNM impressions are usually distributed more randomly. The significant differences in convergence allow a feasible criterion to be set with reference to the convergence tendency so as to collect the more credible CMCs commonly used to distinguish between matching and non-matching impressions.

The density-based spatial clustering of applications with noise (DBSCAN) algorithm is a well-known clustering point algorithm which integrates clusters based on local point density [21]. It requires only the two parameters: Eps and MinPts, where Eps is the neighborhood of a point, and MinPts is the minimum number of points in an Eps. The key idea of this algorithm is that the density in the Eps of a cluster has to meet the given MinPts; that is, the distribution of a cluster is bound to be denser than that of an area of noise. In the improved CMC algorithm, the value of Eps is obtained using a 4-dis function proposed by Ester et al. [21] in which the mean distance of the four nearest points is considered to be the value of Eps. Here, we set the value of Eps as the mean distance of the four nearest cell registration positions that have already been corrected using the LSM method. The mean distance of the cell pair registration positions for the 780 pairs of topographies are depicted in Figure 7. In general, the mean distance of cell registration positions for KM is smaller than 25 pixels, and these values are mostly smaller than those of KNM. Therefore, 25 is chosen as the value of the parameter Eps. The value of MinPts is set at 6 according to the criterion used in the original CMC algorithm [9]. The procedures of DBSCAN for the 780 impression pairs consist of four steps:

1. Select an arbitrary point from the LSM-corrected cell registration position of a pairwise impression;

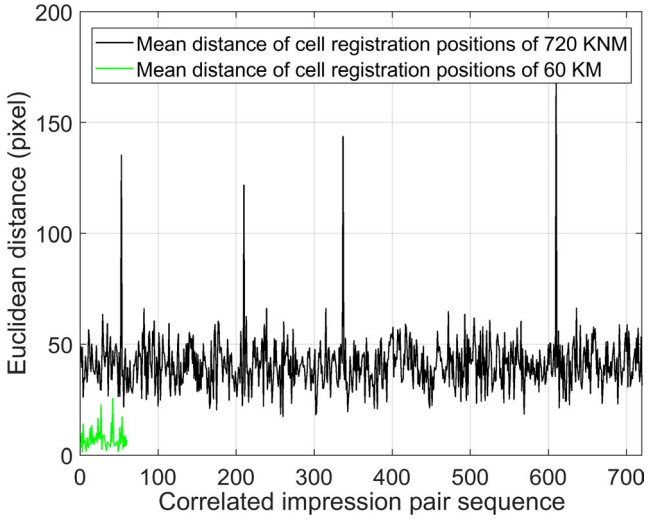

FIGURE 7 Mean distance of cell registration positions. The black line implies a 4-dis mean distance of 720 KNM samples, while the green line implies a 4-dis mean distance of 60 KM samples [Color figure can be viewed at wileyonlinelibrary.com]

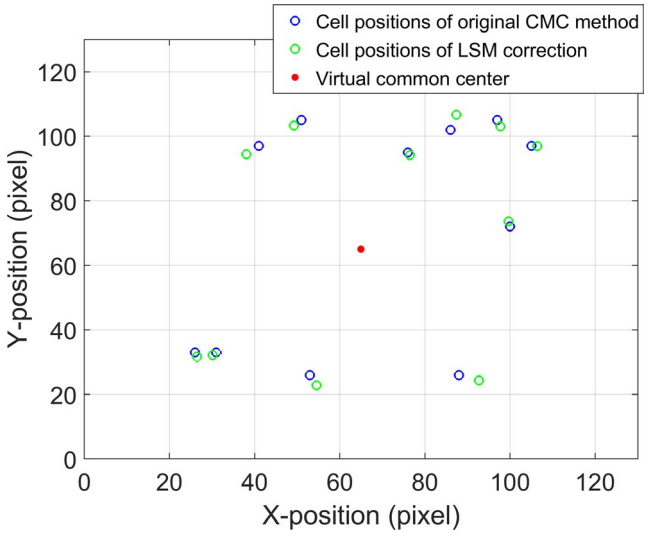

FIGURE 8 Typical divergent distribution of cell registration positions for the pairwise KNM impressions [Color figure can be viewed at wileyonlinelibrary.com]

2. If the number of cell registration positions among the chosen Eps is larger than the MinPts, a cluster is formed, and move to the next point.
3. Repeat step 2 and merge clusters which are density-reachable until all of the points have been processed, i.e., any two clusters which both include at least one of the same points can be merged as a new cluster.
4. Output a cluster of converged cell registration positions or zero.

DBSCAN is useful for registration position clustering because it has few input parameters and can discover clusters irrespective of shape and regardless of whether or not the cluster is convex. In fact, due to the relatively limited number of registration positions

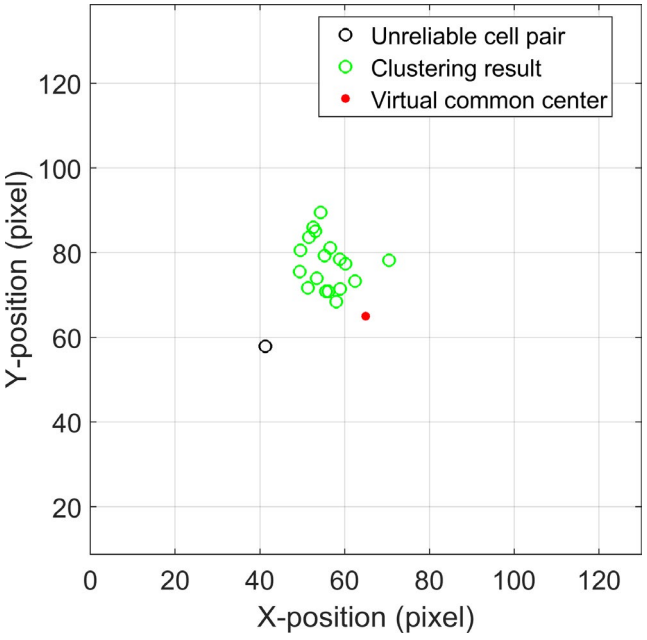

FIGURE 9 Clustering result of cell registration positions for the pairwise KM impressions [Color figure can be viewed at wileyonlinelibrary.com]

and the reasonable setting of the parameters of Eps and MinPts, DBSCAN can usually generate one cluster at most for the determination of CMCs in impression comparison applications. By running the above four steps, if the cell registration positions do not tend to converge and fail to form a cluster (so that the output is zero), the impression pair would be excluded. As shown in Figure 8, although there are more than six congruent cells acquired by the CMC algorithm for the pairwise KNM impressions, their registration positions are obviously divergent. With the DBSCAN algorithm, all the points are not dense enough to form a group, and so it is concluded that the pairwise impression is non-matching. Conversely, for the KM impressions, as shown as in Figure 9, the corrected registration positions show a clear tendency of convergence, and then the density-based clustering algorithm can cluster the positions together and yield a cluster of cells as CMCs. Hence, the clustering method can help the CMC algorithm to exclude independent points, and further ensures the congruence of CMC identification, which is particularly effective in eliminating false positives.

3.5 | Validation tests and results

In order to evaluate the performance of the proposed approaches, validation tests were carried out with a set of 40 firing pin impression samples on cartridge cases fired from 10 pistols of three manufacturers (2 Sig Sauer P226 pistols, 4 Smith&Wesson 9VE pistols, and 4 Ruger P95D pistols). The 40 cartridges are selected from the previous NIST Ballistic Imaging Database Evaluation (NBIDE) project [22]. Sample-to-sample comparisons within this test set include 60 KM and 720 KNM pairs of impressions, giving a total of 780 correlations.

TABLE 1 Process parameters of the convergence-improved CMC algorithm.

Sub-algorithm	Parameters	Actual value	Status
CMC	T_{ACCF}	45%	Optimized
	Rotation increment	15°	Optimized
	Cell size of reference image	50 × 50 pixels	Optimized
	Cell size of comparison image	130 × 130 pixels	Optimized
Areal spline filter	Short cutoff wavelength	5 pixels (7.81 μm)	Arbitrary
Areal Gaussian regression filter	Long cutoff wavelength	60 pixels (93.75 μm)	Optimized
LSM	Correction parameters	Arbitrary	Arbitrary
DBSCAN	Eps	25 pixels distance	Optimized
	MinPts	6 points	Optimized

In practice, the edges of the firing pin impressions which do not contain sufficient individual characteristics are removed first. Then both the reference and comparison impressions are partitioned into 7 × 7 cell arrays. The cell size of the reference impression is set to be square, with approximate dimensions of 50 × 50 pixels (78 × 78 μm) without any overlap, and the larger cell size of the comparison impression is set at 130 × 130 pixels (approximately 202.8 × 202.8 μm). The cell size for the comparison impression offers a large scanned area for the $ACCF_{max}$ value between the correlated cells, thus reducing the influence on the actual $ACCF_{max}$ value of any spatial deviation between corresponding critical features. Furthermore, the large cell size can support a relatively wide rotation increment, which can dramatically decrease rotation times and the burden of cross-correlation calculations between pairs of cells.

The original CMC algorithm and the improved CMC algorithm were run to distinguish between the KM and KNM firing pin topography pairs. In order to better compare their performance, the registration position and orientation thresholds T_x, T_y and T_θ and are removed in all of the approaches, so that each reference cell could be registered to anywhere in the large cell of the comparison impression. For the original CMC algorithm, the rotation parameters are set at a rotation range of 360° in increments of 15° or 3°, and T_{ACCF} =40%. For the improved CMC algorithm, as discussed above, the rotation range is extended to the full 360° range in increments of 15° and registration thresholds set at T_{ACCF} =45%, Eps =25, and MinPts =6. All of the process parameters used are listed in Table 1.

The improved comparison procedures include the following:

1. Remove invalid edge areas and run the Gaussian regression filter on the raw impressions to extract surface roughness.
2. With full rotation range of 360° and 15° increments, run the original CMC algorithm and determine the initial registration positions. These will be used as the tentative key points for further LSM correction.
3. Run LSM algorithm to correct the initial registration positions by improving cross-correlation performance against distortions caused by geometric deformation, depth variation, and angular offset.

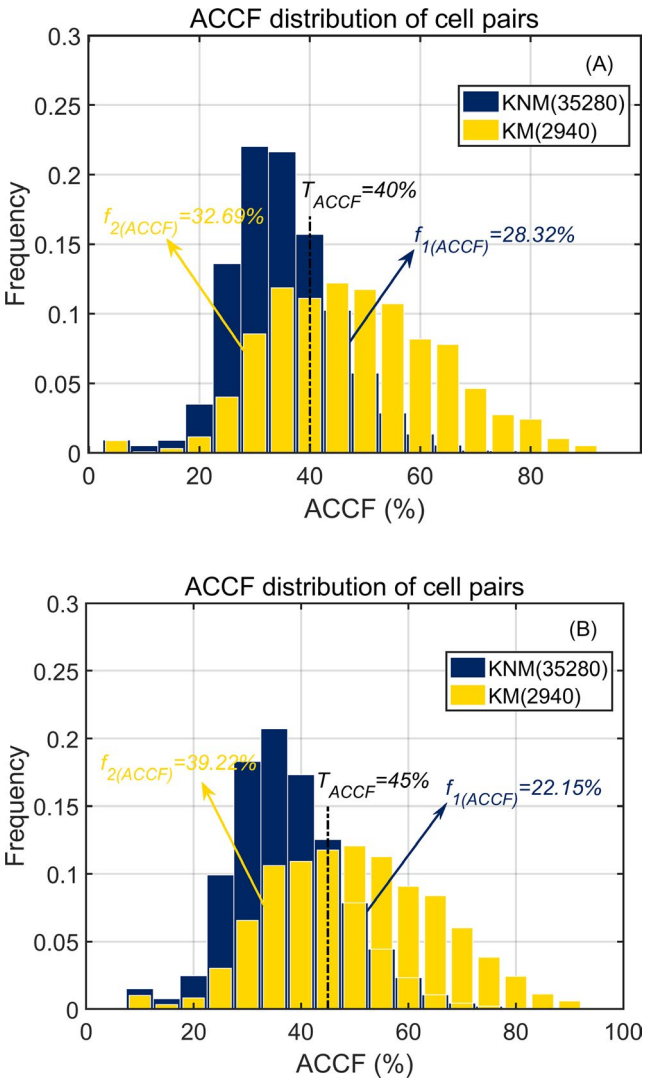

FIGURE 10 distributions of cell pairs in KM and KNM impression correlations acquired using: (A) the original CMC method; (B) LSM correction [Color figure can be viewed at wileyonlinelibrary.com]

4. Perform the DBSCAN method to cluster *x*-*y* registration positions and enhance their congruent distribution pattern. If these registration positions could be identified as a cluster within two

preset thresholds using the DBSCAN approach, then the pairwise impressions are verified as matching.

It should be noted that, as a subsidiary outcome of the LSM correction method, the $ACCF_{max}$ value of each cell pair for both KM and KNM impressions is increased to a certain extent. Figure 10A,B illustrate the distributions of $ACCF_{max}$ values for the KM and KNM correlation cell pairs acquired using the original CMC method and the LSM algorithm respectively. The overlap of the two distributions indicates the closeness between the cell topography similarity of KM and KNM impression pairs when the cell registration location is not constrained by congruency parameters. Certainly, a low degree of overlap makes the separation of KM and KNM impressions easier and reduces the computational burden of congruency evaluation to correctly collect registration cells. The ideal situation is that the frequency of false identifications of cell similarity, $f_{1(ACCF)}$, and the false cell similarity exclusion frequency, $f_{2(ACCF)}$, should both be equal to zero. However, as shown in Figure 10A,B, the two distributions overlap to a considerable extent compared to the ACCF distribution of the breech face impression samples described by Chen et al. [13]. This large distribution overlap also explains why the firing pin impressions are more difficult to examine than other types of impression. In the original CMC algorithm, the suitable value of T_{ACCF} is chosen as 40%, $f_{1(ACCF)}$ = 28.32% and $f_{2(ACCF)}$ = 32.69%. In the improved algorithm, the ACCF threshold is set at 45%, $f_{1(ACCF)}$ = 22.15% and $f_{2(ACCF)}$ = 39.22%. The configuration of $f_{2(ACCF)}$ is slightly larger than $f_{1(ACCF)}$, based on the robust collection capability of the DBSCAN algorithm which can identify reliable registration cell pairs through density clustering disposition. DBSCAN can also guarantee enough CMC number for the KM impressions, even if the number perhaps becomes small constrained by the higher value of T_{ACCF}. At the same time, maintaining a low value of $f_{1(ACCF)}$ is of practical significance in pursuing a lower rate of false-negative identifications.

As shown in Figure 11, the original CMC algorithm shows a large overlap between the CMC distributions of the KM and KNM pairs. Therefore, it is impossible to completely distinguish between KM and KNM firing pin impressions, as the algorithm yields high probabilities of false positive and false-negative results. Figure 11A indicates that, for the original CMC method with a rotation increment of 15°, the CMC distribution range is 6–30 for the 60 KM impression pairs, and the CMC distribution range is 2–7 for the 720 KNM impression pairs. As shown in Figure 11b, with a rotation increment of 3°, the CMC distribution range is 3–20 for the 60 KM pairs and 1–5 for the 720 KNM pairs. It can be seen that the rotation increment adjustment fails to improve the original CMC method to identify KM from KNM pairs. As discussed above, this is mainly because the geometric deformation of firing pin impressions alters the distributions of micro-feature in the correlated topographies and affects the identification accuracy of KM pairs.

Figure 12 compares the results using Chen's method [13] and our improved algorithm, revealing a significant enhancement in computer-based discrimination ability. Chen's method actually implements the CMC method to search the initial matching

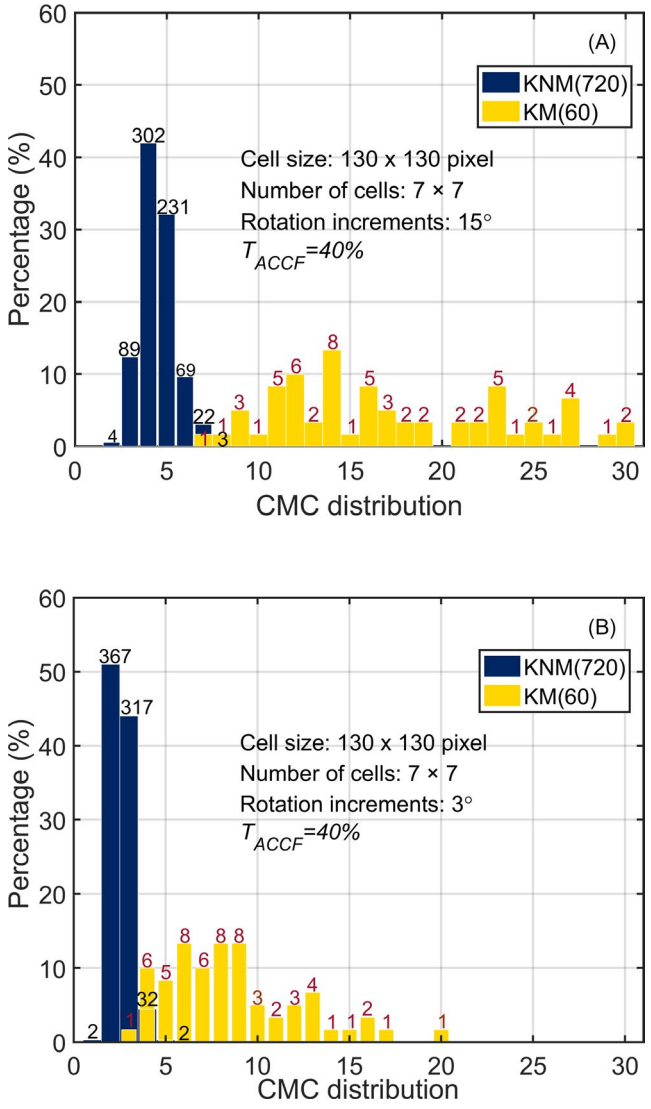

FIGURE 11 CMC distribution of impressions using the original CMC algorithm with a rotation increment of: (A) 15° and (B) 3° [Color figure can be viewed at wileyonlinelibrary.com]

impressions and further takes advantage of the convergence feature to remove the unreliable matching cell pairs included in CMCs. Chen et al. (13) also report validation experiments which show that their method can effectively match breech face impressions. Unfortunately, our experiments show that this method is not suitable for the comparison of firing pin impressions due to their specific geometric and depth distortions. As shown in Figure 12A, Chen's method disposes of KNM impressions well and controls all their CMCs within 1–3. But it is obviously that this method can also reduce the CMCs of KM impressions, thereby misidentifying some KM pairs as mismatches.

Compared to Chen's method, our improved method focuses on improving the correlation accuracy and registration position of each cell pair, so as to enhance the reliability and accuracy of the entire comparison algorithm. As shown in Figure 12B, the improved method successfully separates the distribution of the CMC scores of KM and KNM pairs, and does not produce any false identifications or

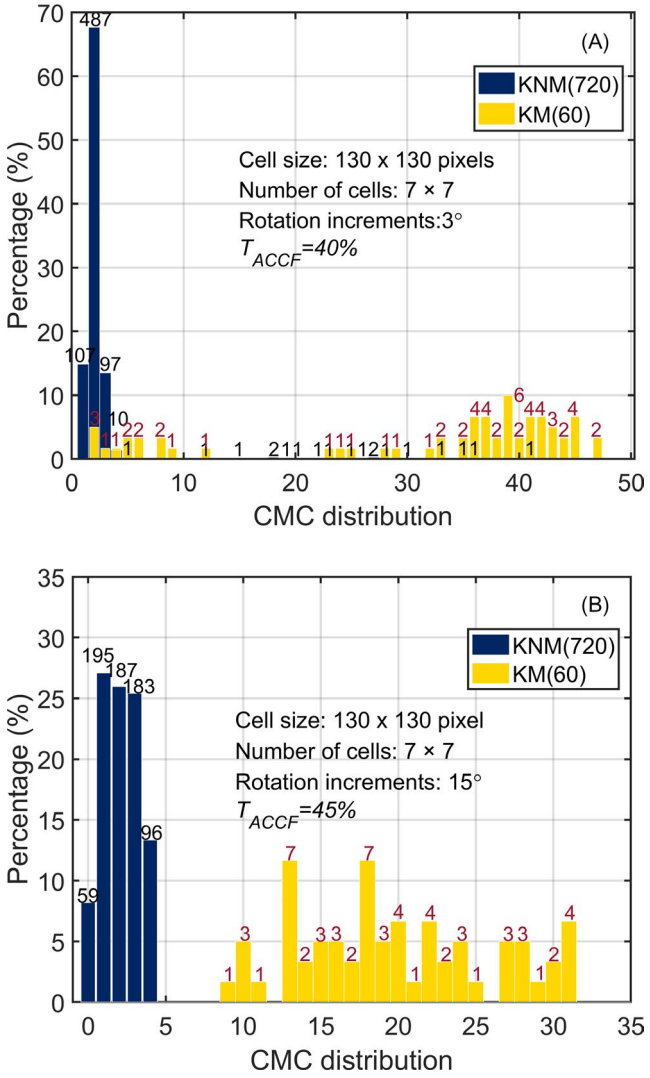

FIGURE 12 CMC distribution of impressions using: (A) Chen's method and (B) the improved CMC algorithm [Color figure can be viewed at wileyonlinelibrary.com]

false exclusions. For the 60 KM pairs, where the threshold value of $T_{(ACCF)}$ = 45%, the CMC distribution histograms range from 9 to 31, and for the 720 KNM images the CMC distribution histograms range from 0 to 4. Furthermore, approximately 82% KNM pairs with CMCs are less than 3. This indicates that the improved method yields fewer CMCs for KNM pairs. These improvements are attributed to the performance of the LSM and DBSCAN combination algorithms. The LSM algorithm can correct the *x-y* registration positions of the correlated cell pairs, enhancing the accuracy of their correlation. Meanwhile, the DBSCAN algorithm can remove the pseudo congruent matching cells by use of convergence tendency of the cell registration positions, and acquire more reliable CMCs.

4 | SUMMARY

The firing pin impression on a cartridge case is one of the most important signatures in firearms identification in forensic science. In this paper, we attempt to improve the original CMC method based on a convergence feature and develop practical convergence-improved algorithms for the automated comparison of firing pin impressions.

For the special concave shape of firing pin impressions, the areal Gaussian regression filter is applied to extract a high-frequency roughness as the individual characteristics for further pairwise discrimination. The CMC algorithm is conducted in the full range of rotation with a relatively large increment to achieve actual automated comparison without prior empirical estimation of the possible matching angle. Then LSM, which is a highly accurate patch matching method, is introduced to overcome distortions in the correlations between pairs of cells caused by geometric deformations of hemispherically shaped impressions and the incremental rotation of the CMC algorithm. With reference to the different patterns of convergence between correlated KM and KNM cell pairs, a density-based clustering algorithm is employed to cluster the dense *x-y* registration positions relative to a virtual common center and to yield more reliable CMCs.

The proposed comparison algorithm is validated using 780 correlations originating from a set of 40 cartridge cases fired from 10 pistols. The KM and KNM topography pairs were correctly identified based on the values of three parameters set at $T_{(ACCF)}$ = 45%, Eps =25 and MinPts =6, with no false identifications or false exclusions for these topographies. In contrast with that of the original CMC method, the performance of the improved CMC method for the comparison of firing pin impressions is significantly enhanced. Even though the data set used in this study is of limited size and was collected from specific types of firearms and ammunition, the proposed method could be applied to a larger data set.

It should be noted that the improved CMC method can perform well in comparing general firing pin impressions but, like the original CMC method, could not handle broken impressions. Hence, further data processing algorithms for use in the CMC method will need to be developed in the future to recover the broken data. In addition, the improved algorithm includes some critical parameters that could affect its overall comparison performance. The setting of parameters may not be optimal in the current algorithm, and their optimization would also require the use of a larger database.

ACKNOWLEDGMENTS

The authors are grateful to the High Performance Computing Center of Nanjing Tech University for supporting the computational resources.

REFERENCES

1. Chu W, Thompson RM, Song J, Vorburger TV. Automatic identification of bullet signatures based on consecutive matching striae (CMS) criteria. Forensic Sci Int. 2013;231:137–41. https://doi.org/10.1016/j.forsciint.2013.04.025.
2. Zhang H, Gu J, Chen J, Sun F, Wang H. Pilot study of feature-based algorithm for breech face comparison. Forensic Sci Int. 2018;286:148–54. https://doi.org/10.1016/j.forsciint.2018.02.026.
3. Xie F, Xiao S, Blunt L, Zeng W, Jiang X. Automated bullet-identification system based on surface topography techniques.

Wear. 2009;266(5–6):518–22. https://doi.org/10.1016/j.wear.2008.04.081.
4. Ott D, Thompson RM, Song J. Applying 3D measurements and computer matching algorithms to two firearm examination proficiency tests. Forensic Sci Int. 2017;271:98–106. https://doi.org/10.1016/j.forsciint.2016.12.014.
5. Vorburger TV, Song J, Petraco N. Topography measurements and applications in ballistics and tool mark identifications. Surf Topogr. 2015;4(1):013002. https://doi.org/10.1088/2051-672X/4/1/013002.
6. Forensic Technology Inc. http://www.ultra-forensictechnology.com/. Accessed 21 Jun 2020
7. Gerules G, Bhatia SK, Jackson DE. A survey of image processing techniques and statistics for ballistic specimens in forensic science. Sci Justice. 2013;53(2):236–50. https://doi.org/10.1016/j.scijus.2012.07.002.
8. Yammen S, Muneesawang P. Cartridge case image matching using effective correlation area based method. Forensic Sci Int. 2013;229(1):27–42. https://doi.org/10.1016/j.forsciint.2013.03.015.
9. Tong M, Song J, Chu W, Thompson RM. Fired cartridge case identification using optical images and the congruent matching cells (CMC) method. J Res Natl Inst Stand Technol. 2014;119:575–82. https://doi.org/10.6028/jres.119.023.
10. Peralta D, Galar M, Triguero I, Paternain D, Garcia S, Barrenechea E, et al. A survey on fingerprint minutiae-based local matching for verification and identification: taxonomy and experimental evaluation. Inf Sci. 2015;315:67–87. https://doi.org/10.1016/j.ins.2015.04.013.
11. Valdes-Ramirez D, Medina-Pérez MA, Monroy R, Loyola-González O. A review of fingerprint feature representations and their applications for latent fingerprint identification: trends and evaluation. IEEE Access. 2019;7:48484–99. https://doi.org/10.1109/ACCESS.2019.2909497.
12. Song J. Proposed NIST ballistics identification system (NBIS) based on 3D topography measurements on correlation cells. AFTE J. 2013;45(2):184–94.
13. Chen Z, Song J, Chu W, Soons JA, Zhao XZ. A convergence algorithm for correlation of breech face images based on the congruent matching cells (CMC) method. Forensic Sci Int. 2017;280:213–23. https://doi.org/10.1016/j.forsciint.2017.08.033.
14. Song J, Chu W, Tong M, Soons J. 3D topography measurements on correlation cells: a new approach to forensic ballistics identifications. Meas Sci Technol. 2014;25(6):064005. https://doi.org/10.1088/0957-0233/25/6/064005.
15. Zhang H, Song J, Tong M, Chu W. Correlation of firing pin impressions based on congruent matching cross-sections (CMX) method. Forensic Sci Int. 2016;263:186–93. https://doi.org/10.1016/j.forsciint.2016.04.015.
16. International Organization for Standardization. ISO 16610–71:2014. Geometrical product specifications (GPS)-filtration-part 71: Robust areal filters: Gaussian regression filters. Geneva, Switzerland: International Organization for Standardization; 2014.
17. Song J. "Proposed congruent matching cells (CMC) method" for ballistics identification and error rate estimation. AFTE J. 2015;47(3):177–85.
18. Tong M, Song J, Chu W. An improved algorithm of congruent matching cells (CMC) method for firearm evidence identifications. J Res Natl Inst Stand Technol. 2015;120:102–12. https://doi.org/10.6028/jres.120.008.
19. Ackermann F. Digital image correlation: performance and potential application in photogrammetry. Photogramm Rec. 2010;11(64):429–39. https://doi.org/10.1111/j.1477-9730.1984.tb00505.x.
20. Li Z, Wang J. Least squares image matching: a comparison of the performance of robust estimators. ISPRS Annals Photogramm Remote Sens Spat Inf Sci. 2014;2(1):37–44. https://doi.org/10.5194/isprsannals-II-1-37-2014.
21. Ester M, Kriegel HP, Sander J, Xu XW. A density-based algorithm for discovering in large spatial databases with noise. In: Simoudis E, Han J, Fayyad U, editors. Proceedings of the Second International Conference on Knowledge Discovery and Data Mining; Portland, OR. Menlo Park, CA: AAAI; 1996. p. 226–31.
22. Vorburger TV, Yen J, Bachrach B, Renegar TB, Filliben J,Ma L, et al. Surface topography analysis for a feasibility assessment of a National Ballistics Imaging Database. NISTIR 7362. Gaithersburg, MD: NIST; 2007. p. 27–40.

How to cite this article: Zhang H, Zhu J, Hong R, Wang H, Sun F, Malik A. Convergence-improved congruent matching cells (CMC) method for firing pin impression comparison. *J Forensic Sci*. 2021;66:571–582. https://doi.org/10.1111/1556-4029.14634